Baghdad Science Journal

Volume 23 | Issue 2 Article 4

2-23-2026

Synthesis, Characterization and Photodegradation Study of Titanium Dioxide Nanoparticles Mediated Using Melon Peel Extract

Mohamed Abdelkalik Hussain
Department of Chemistry, College of Science, University of Baghdad, Baghdad, Iraq,
muhamedabdelkalik@gmail.com

Wadhah Naji Al Sieadi
Department of Chemistry, College of Science, University of Baghdad, Baghdad, Iraq,
wadhah.n@sc.uobaghdad.edu.iq

How to Cite this Article

Hussain, Mohamed Abdelkalik and Sieadi, Wadhah Naji Al (2026) "Synthesis, Characterization and Photodegradation Study of Titanium Dioxide Nanoparticles Mediated Using Melon Peel Extract," *Baghdad Science Journal*: Vol. 23: Iss. 2, Article 4.
DOI: https://doi.org/10.21123/2411-7986.5196

BAGHDAD SCIENCE JOURNAL 2026;23(2):447–461

Scan the QR to view the full-text article on the journal website

RESEARCH ARTICLE

Synthesis, Characterization and Photodegradation Study of Titanium Dioxide Nanoparticles Mediated Using Melon Peel Extract

Mohamed Abdelkalik Hussain *, **Wadhah Naji Al Sieadi**

Department of Chemistry, College of Science, University of Baghdad, Baghdad, Iraq

ABSTRACT

The importance of nanotechnology in protecting the environment is represented in multiple applications, including, for example, the green synthesis of nanoparticles (NPs), using the remains of plant parts, as well as photolysis application that used semiconductors NPs which showed a clear effect in treating water from organic pollutants, this study combines these two applications, in terms of green synthesis of titanium dioxide nanoparticles (TiO_2NPs) using melon peel (*Cucumis melo L.*) in sol-gel method, as well as, the photodegradation of methylene blue dye (MB) by using a new irradiation photoreactor device which has designed and implemented for this purpose. This device used to irradiate MB dye with three different types of ultraviolet−visible (UV) light sources to study the photodegradation with different cases, first on circulation of MB dye only, second when irradiation MB dye with UV-A, UV-B, UV-C light sources with circulation, finally, the effect of adding (0.05 g) of green synthesized of TiO_2NPs by using melon peel extract in sol-gel method with irradiation and circulation MB dye in the system. Different percentage of MB dye removal where reported. The prepared of TiO_2NPs catalysts were characterized using, Energy dispersive analysis (EDX), Ultraviolet−visible spectroscopy (UV-Vis), Scanning electron microscope (SEM), Fourier transform infrared spectroscopy (FTIR), X-ray spectroscopy (XRD), Atomic force microscopy (AFM). High performance of photodegradation was absorbed under UV-C, UV-B irradiation of MB dye in 90 min.

Keywords: Green synthesis, Melon peel, Methylene blue dye, Photodegradation, Titanium dioxide nanoparticle

Introduction

Nanotechnology field refers to special branch which get great hope to scientific career, molecular manufacturing, applications, devices at nanoscale.[1] Nanomaterials are materials or molecules which have at least one dimensional between 1 and 100 nanometers with unique and interesting properties.[2,3]

Metal nanoparticles have large surface area and small particle size compared with their counterparts in non-nano compounds, these particles are characterized by different characteristics depending on their geometry and morphology and therefore have different physical and chemical properties from bulk, and thus, they had wide applications in several fields in electronics, agriculture, biomedical, medicines, environment.[4,5]

The production of nanomaterials traditionally involves two approaches, physical and chemical methods, physical methods such as pulsed laser ablation, mechanical milling fabrication method, and sputtering fabrication method,[6] these methods are superior to chemical approaches in terms of solvent contamination, yield consistent monodisperse nanoparticles.[7] Chemical approaches such as sol-gel method, molecular condensation, chemical vapor deposition and

Received 21 April 2024; revised 20 September 2024; accepted 22 September 2024.
Available online 23 February 2026

* Corresponding author.
E-mail addresses: muhamedabdelkalik@gmail.com (M. A. Hussain), wadhah.n@sc.uobaghdad.edu.iq (W. N. A. Sieadi).

https://doi.org/10.21123/2411-7986.5196

chemical reduction,[8] used organic solvents exceedingly which has a big concern to environment due to the production of carbon dioxide.[9,10]

In the current development of nanomaterials, green synthesis methods are gaining great attention with its application of minimization of waste,[11,12] environment friendliness,[13,14] avoiding the production of unwanted products,[15–17] eco-friendly synthesis procedures with using natural resources such as (leaves, seeds, and flowers)[18,19] or microorganisms (yeasts,[20] bacteria,[21] and fungi[22]), containing bioactive agents, responsibility of the green synthesis of metal nanoparticles.[23,24]

Plants in nature contain bioactive compounds, such as flavonoid,[25] alkaloid,[26] sugar,[27] polyphenol,[28] organic acid,[29] terpenoid,[30] antioxidant.[29] These bioactive compound role as reduction agents in the synthesis of nanomaterials procedure as electron donors or capping agent.[31]

Scientific community had interest in natural antioxidants, Melon (*Cucumis melo L.*) belongs to the Cucurbitaceae family that is inclusive of several fruit species, which is considered one of the most exported fruits worldwide, peel and seeds.[32] In last ten years, there was 30 million tons of melon's annual production, which consumed traditionally.[33] Also, melons are known for their medicinal features, it has been found that extracts of the Cucurbitaceae family have antibacterial, antifungal, wound-healing, antiviral, antidiabetic (type 2), antidiarrheal, and anti-inflammatory activities,[32,34] with industrial processing of melon, large waste products from seeds and peel are produced which threaten the environment. It's vital to re-used these residues which are rich sources of active compounds such as vitamins, dietary fibers, polyphenols, enzymes. Hence, it is of great interest as there is an increased demand for natural compounds.[35] There are several reports that have studied the green synthesis of metal nanoparticles using melon peel.[36,37]

Photocatalytic technology is considered one of the most environmentally-friendly water treatment from organic pollutants, using semiconductors that does not require additional chemicals, with renewable energy (solar energy) to degrading organic pollutants.[38,39] TiO_2NPs are known as best semiconducting substance with unique chemical, optical, and electronic properties,[40] TiO_2-NPs are known with high chemical stability, low cost, non-toxicity, high photocatalytic activity, and environmental friendliness.[41]

The present work reports the photocatalytic degradation of MB dye by green synthesized TiO_2NPs as a photocatalyst using melon peel extract under irradiation of different UV light source which are, UV-A, UV-B, and UV-C in new designed photoreactor. A comparative photocatalytic activity of TiO_2NPs was investigated, along with their reaction kinetics.

Materials and methods

Chemicals and materials

Methylene blue ($C_{16}H_{18}ClN_3S.xH_2O$) was bought from Merck (≥95%). Titanium tetrachloride ($TiCl_4$) (99.99%) was supplied from Sigma–Aldrich, while ammonia solution was obtained from Prolabo (≥98%), deionized water had been used through the study.

Preparation of melon peel aqueous

Melon peel bought from market, the peels are collected and washed by distilled water to remove all remaining parts, the peels has been dried in oven for several days, the dried peels have been ground to powder using grinder model HM-917, 220-240 V, from Al saif-electric, China. 5 g of melon powder was added to 100 ml DW, then the mixture was heated using stirrer hot plate type cimarec model MA-187, China, the temperature kept under 60 °C, with stirring for 25 min, a yellow solution was obtained, this mixture was cooled down at room temperature, filtered, stored in dark place for later use in green synthesis of TiO_2NPs.

Preparation of green TiO_2 NPs by the sol-gel

To synthesize TiO_2NPs with sol-gel method as showed in Fig. 1, 50 ml of 0.5 M $TiCl_4$ was mixed with 50 ml of melon peel yellow juice, the mixture was boiled to 60 °C with stirring, then, ammonia solution10 ml was added dropwise, a white solution was obtained which was centrifuged to precipitate the sold. Then it was filtered and dried in an oven with hot air for 24 hours, then using crystal mortar to grind the TiO_2NPs to powder. Finally, a purification was carried out to gain TiO_2NPs powder, at high temperature (400 °C) using calcination furnace to remove water as absorbed moisture for a period of 3-4 hours to oxidize the entire substance, a clear white powder was obtained, Fig. 1. The TiO_2NPs are characterized by AFM, SEM, FTIR, UV-Vis spectrum, XRD, and EDAX.[42]

Photoreactor and UV light sources

A homemade photoreactor system was designed to this procedure Fig. 2, with using inset killer frame bought from market, and instead of using common stirrer hot plate, a water diaphragm pump with 650-750 mt rated flow 0.3 A was attached to the frame. An ultraviolet visible UV lamp chamber was bought from

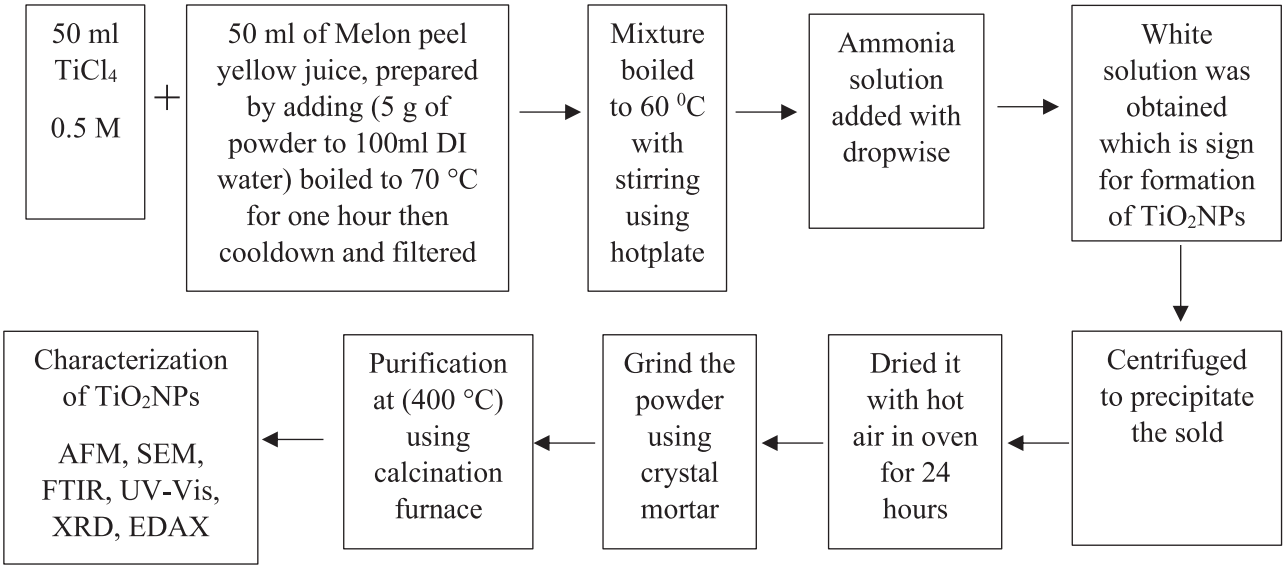

Fig. 1. TiO_2NPs green synthesis steps by the Sol-Gel method.

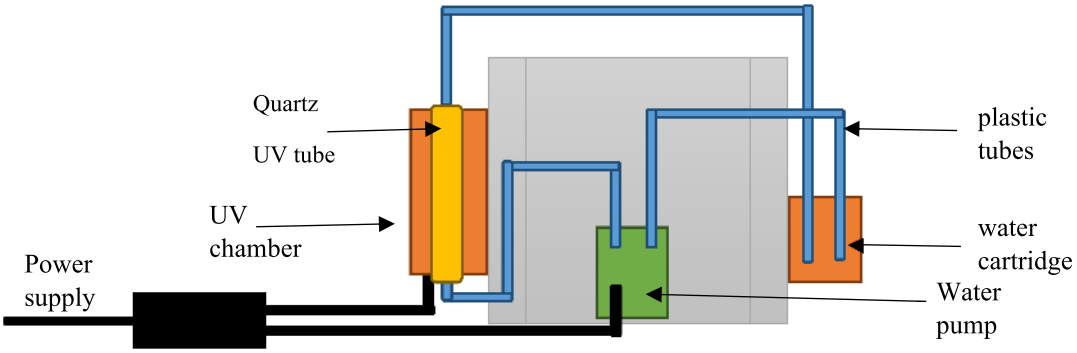

Fig. 2. Homemade photoreactor system.

market and connected to the frame, to close the circle of flowing, a water cartridge with 10 inches was used, plastic tubes connecter from water purifier were used, the UV-light source used are, (T5 8W) UV-A (365 nm), (T5 8W) UV-B (311 nm), (T5 8W), UV-C (254 nm), all UV-light sources were bought from coospider Quartz UV-Lamp, 220 v, China.

Photodegradation procedure

The amount of solution needed for the new photoreactor system has been measured, 320 ml of MB dye with concentration of 6×10^{-6} M and pH = 6.4 was chosen. First set of experiments was conducted to study the circulation effect on MB dye in the system without any irradiation or loading TiO_2NPs, second set of experiments was conducted to study the irradiation effect with UV-A, UV-B, and UV-C on MB dye without loading TiO_2NPs. Last set of experiments were carried out with loading TiO_2 NPs powder, A 0.05 g was added to the system to study the effect of adding TiO_2NPs with irradiation using lamps UV-A, UV-B, and UV-C on MB dye degradation. To ensure the adsorption–desorption equilibrium of MB dye on the surface of the photocatalyst, the solution was kept in a dark place for 15 min, all experiments were conducted in 90 min. The first sample 2.5 ml was collected from the system before the irradiation start, when irradiation started, the sample was collected every 15 min by using 1ml pipette, all samples were centrifuged at 4000 rpm, before using UV-Vis double beam spectrophotometer.[43]

Photodegradation kinetic study

The photocatalytic study of TiO_2NPs was tested, the photodegradation rate of MB dye was calculated by using the following Eq. (1)[44,45]:

$$\text{MBDegradation}\,(\%) = \frac{A0 - At}{A0} \times 100 \qquad (1)$$

Where A0 is the absorbance of initial MB; At is the absorbance of the solution after irradiation at time t. According to first order kinetics reaction, rate constant k (min^{-1}) was determined by using the following relation Eq. (2)[46,47]:

$$\ln\left(\frac{C_t}{C_0}\right) = -kt \quad (2)$$

Where C0 and Ct are concentration at the beginning and at a certain time, t is the irradiation time.

Characterization of titanium oxide nanoparticles

The mean diameters of TiO_2NPs and surface roughness are measured by atomic force microscopy (NaioAFM 2022 model, Nanosurf AG, Switzerland). Environmental scanning electron microscopy (ESEM) and Energy-dispersive, X-ray spectroscopy (EDX) for elemental analysis were carried out using a Tescan Mira 3 (French) with resolution 1.2 nm at 30 kV; 2.3 nm at 3 kV. An X-ray diffractometer (XRD)was used for identifying the composition and structure of TiO_2NPs from persee China, XD3, operating conditions of 60 kV and 50 mA from range -40-90° at a scanning speed 0.125°-120°/ min, step size of 0.00025° with scanning radius 180mm. To measure the absorbances MB dye, a BOYN double-beam BNUV-D8000 UV−Vis spectrophotometer (China) was used. To identify the compounds functional groups, a Fourier transform infrared spectroscopy (FTIR) analysis was performed using a Vertex-80v FTIR spectrometer connected to a Hyperion 3000 IR microscope (Bruker Optics GmbH, Germany), frequency range 4000–400 cm^{-1}.

Results and discussion

Morphological analysis

Scanning electron microscope and energy dispersive analysis X-ray

The green synthesis TiO_2NPs was characterized by Scanning Electron Microscope (SEM) analysis to study the surface morphology, the results showed TiO_2NPs with an average size of 39 nm with high surface area, Fig. 3a, also the prepared TiO_2NPs showed slight agglomerations due to high calcinations temperature 400 °C to accelerate crystal growth of TiO_2NPs Fig. 3b, as calcination aim to eliminate water content, and change the structure of TiO_2NPs from amorphous to crystalline which was accompanied by phase transformation from anatase to rutile phase.[48,49]

Energy dispersive X-ray analysis (EDAX) for prepared TiO_2NPs as in Fig. 4, shows high peak of titanium with high KeV. Table 1. describes the composition and different elements in terms of weight percentage (Wt. %) and atomic percentage (At%), different elements appeared from the composition compounds of melon peel role in green syntheses procedure of TiO_2NPs.

Table 1. Chemical composition of green TiO_2NPs in terms of weight and atomic percentage from (EDAX) measurement.

Elements	Weight percentage (Wt. %)	Atomic percentage (At %)
C	5.47	10.30
O	45.24	63.97
Mg	2.27	2.11
Si	1.83	1.47
P	2.49	1.82
Ca	1.60	0.90
Ti	41.1	19.41
Total	100.00	100.00

X-ray diffraction (XRD)

The structure and crystalline of prepared TiO_2NPs were done by X-ray diffraction using Cu-Kα diffractometer X-rays, (λ) 1.5406 Å, 2θ range of 10° to 80° step size of 0.00025°.

Fig. 5, shows sharp spectrum with diffraction peaks appeared at 2θ = 27.73°, 36.25°, 41.45°, 44.23°, 54.55°, 56.42°,63.0°, and 69.60°, these results are identical with rutile phase patterns of TiO_2NPs from (JCPDS file 96-900-9084),[50,51] with tetragonal crystal planes with average crystallite size for the rutile TiO_2NPs estimated according to the Debye−Scherrer's Eq. (3)[52]:

$$D = \frac{K * \lambda}{\beta * \text{Cos}\,\theta}. \quad (3)$$

Where D is NPs crystalline size, K e represents the Scherrer constant (0.94), λ is the X-ray wavelength, β is the peak width at half maximum, and θ is the Bragg's diffraction angle. The average particle size has been calculated to be (12.7 nm) as shown in Table 2.

FTIR spectroscopy study

To determine the main functional groups of TiO_2NPs with Melon peel powder, an FTIR spectroscopy was used for both, melon peel and green synthesis TiO_2NPs powder as shown in Fig. 6a and Fig. 6b. The spectra absorption from the range of 4000–400 cm^{-1}, with several spectrum peaks, indicates high purity product formation of TiO_2NPs. Peaks were observed around 3442.70 cm^{-1}, and 3423.41 cm^{-1} are attributed to O–H symmetric and asymmetric stretching vibrations of the hydroxyl groups (Ti-OH).[53]

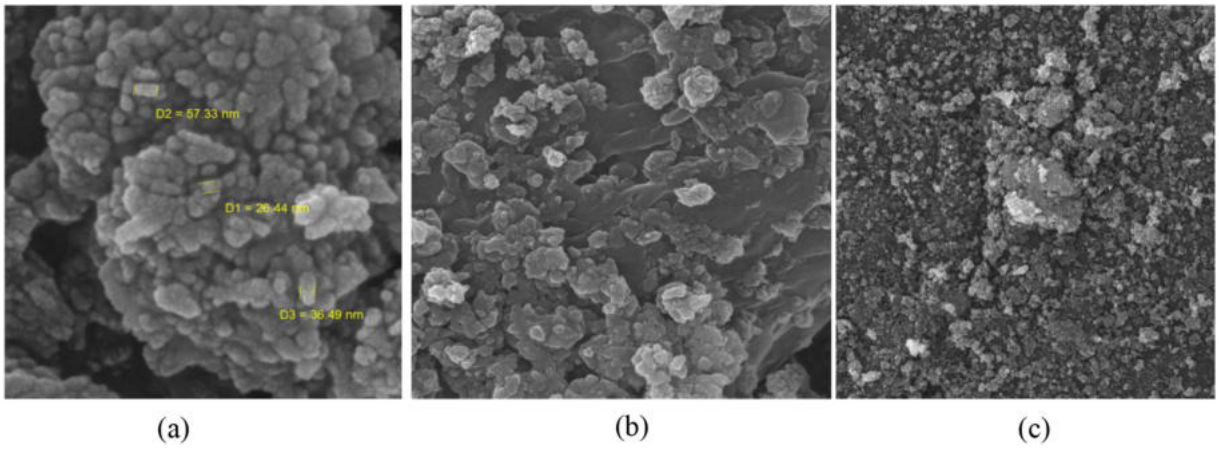

Fig. 3. SEM images of TiO_2NPs view field (a) 200 nm, (b) 1 μm, (c) 5 μm.

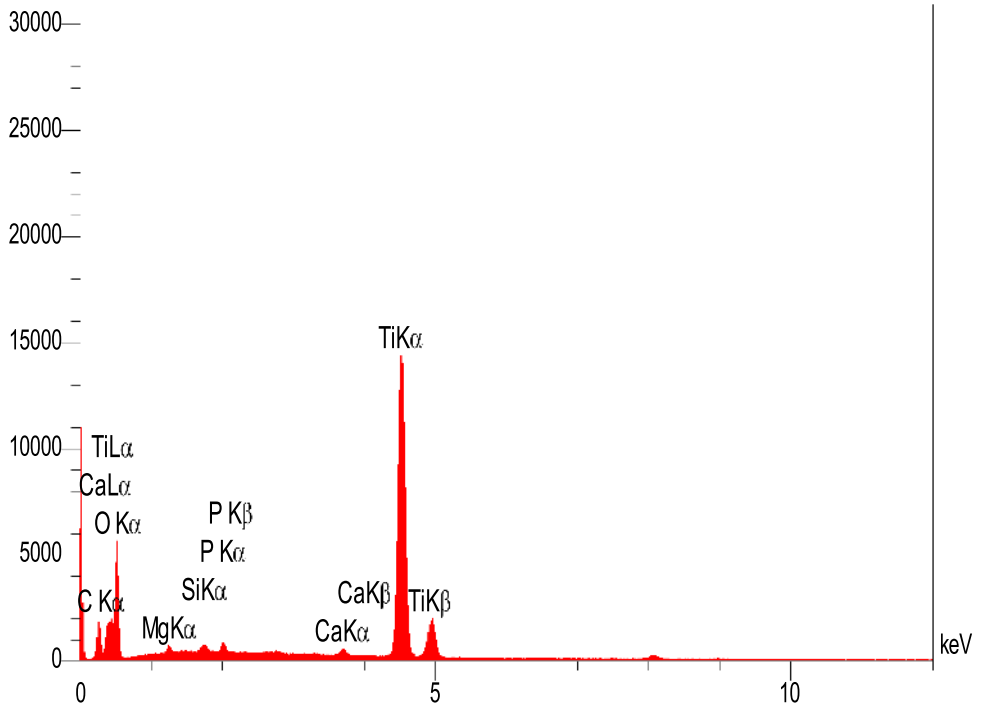

Fig. 4. EDAX spectrum (Energy dispersive analysis of X-ray) of green TiO_2NPs.

Table 2. TiO_2NPs Crystallite size calculation.

2theta (deg)	d[A]	I/I0	counts	FWHM total	FWHM instr.	FWHM sample	Correlated phase(s)	Crystallite size
27.73	3.2150	1000.0	325	1.4436	0.2050	1.2385	Rutile	69.1
36.25	2.4761	478.4	120	1.1154	0.7210	0.3944	Rutile	221.6
36.28	2.4745	145.5	37	1.1388	0.7222	0.4168	Rutile	209.7
41.45	2.1767	327.6	88	1.1970	0.7413	0.4557	Rutile	194.8
44.23	2.0463	89.8	28	1.3670	0.7006	0.6665	Rutile	134.5
54.55	1.6809	614.5	207	1.4968	0.8543	0.6425	Rutile	145.4
56.42	1.6294	140.0	57	1.8169	1.0553	0.7616	Rutile	123.7
63.00	1.4743	135.4	68	2.2409	0.8444	1.3965	Rutile	69.7
69.60	1.3497	232.6	123	2.3429	0.6385	1.7044		59.3
				Average crystallite size calculated from peaks/lines = 127.3 A				

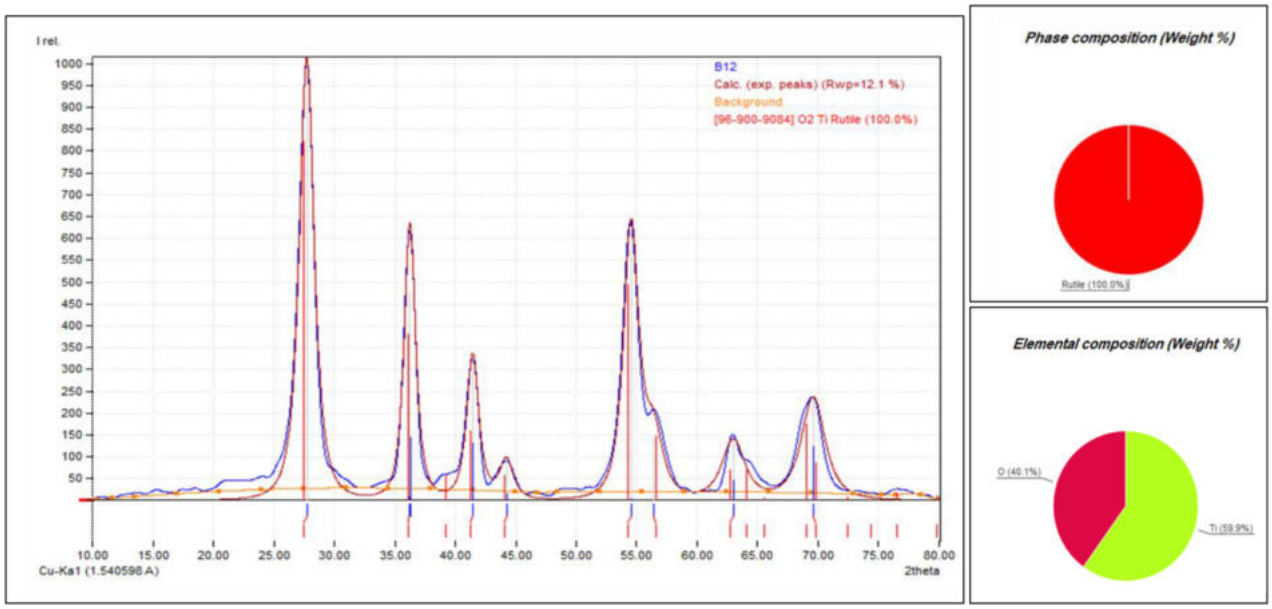

Fig. 5. XRD pattern of green synthesis TiO_2NPs.

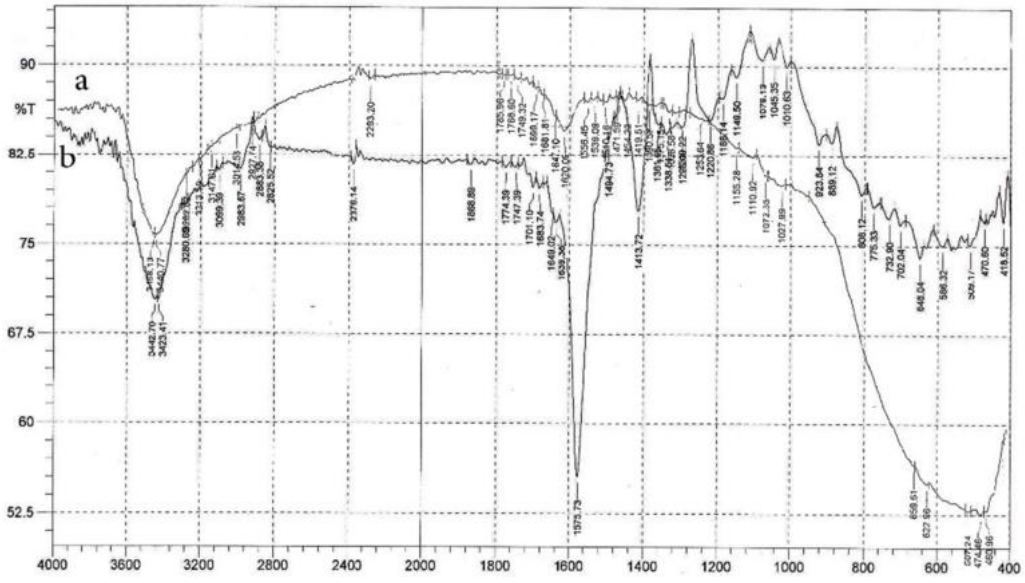

Fig. 6. FTIR pattern (a) green synthesis TiO_2NPs (b) melon peel.

The observed peaks at 1575 cm^{-1} are attributed to (C=O) stretching vibrations groups. The peaks observed at 1413.72 cm^{-1} can be attributed to the C-H bending. For the pure TiO_2, it was reported that the peaks at the broad band from 800 to 400 cm^{-1} region is attributed to the Ti-O stretching and Ti-O-Ti vibration absorption from the anatase TiO_2NPs.[54,55]

Atomic force microscopy (AFM)

The TiO_2NPs phase's topography was analyzed by AFM, which offers a large microstructural arrays surface inspection. Fig. 7 shows the (3D) image with for TiO_2NPs.

Table 3. shows surface average roughness (surface area: 6.830 nm), root mean square (RMS), with small average median (10.21 nm), which can be can observed as one significant parameter.

Photodegradation studies

Absorption of MB dye

The concentration of experimental part chosen was 20ppm (6×10^{-5} M) at 662 nm wave length and

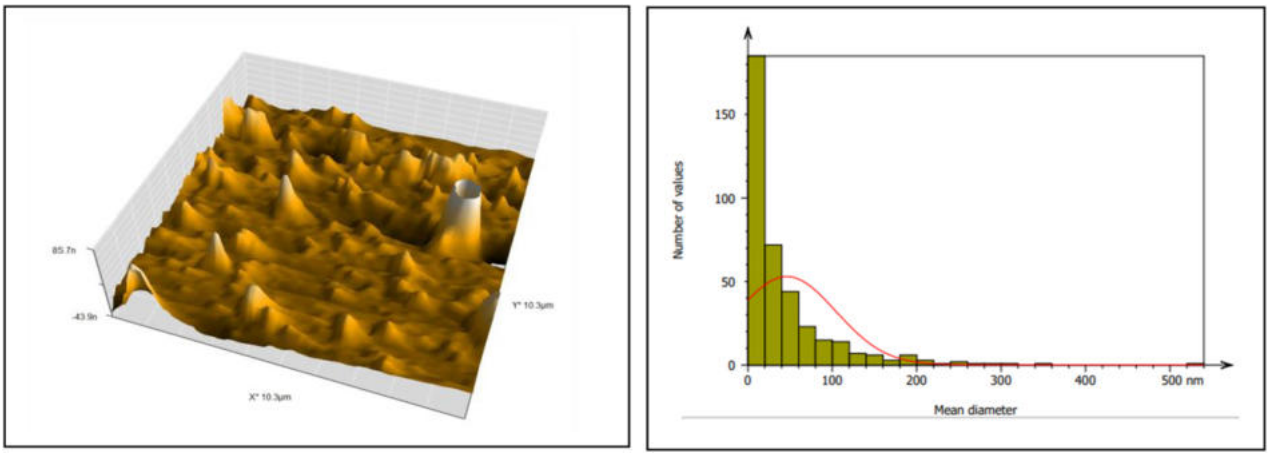

Fig. 7. Atomic force microscopy analysis of TiO_2NPs.

Table 3. Average mean diameter, root mean square.

Parameters	Projected area nm^2	Mean diameter nm	Z-maxima nm
Particle 1	672.7	14.76	6.830
Particle 2	672.7	14.76	6.831
Particle 3	672.7	14.76	6.836
Particle 4	672.7	14.76	6.853
Particle 5	672.7	14.76	6.858
Global statistics			
Mean	5595	45.97	10.21
Min	189.2	9.611	6.830
Max	263570	522.2	47.66

0.680 absorbance, by reference to Beer's law, this concentration of 20ppm which lies between 0.2-0.7 absorbances is with least errors and the best range for measurements.[56]

To study the absorption of MB dye by TiO_2NPs surface in the visible light region, (0.05 g) of TiO_2NPs was added to 20 ppm (320 ml) of MB dye and exposed to sun light. From results in Fig. 8, it is clear that TiO_2NPs suffers from low light absorption in the visible region, because of large bandgap of TiO_2NPs with 3.0 eV.[57]

Although TiO_2NPs has potential as most efficient semiconductor in photocatalysis due to optical and electronic properties for removing organic substances from contaminated water, but it suffers from low quantum yield and low light absorption region because of its wide bandgap, to overcome those issues, several modification of TiO_2NPs were required

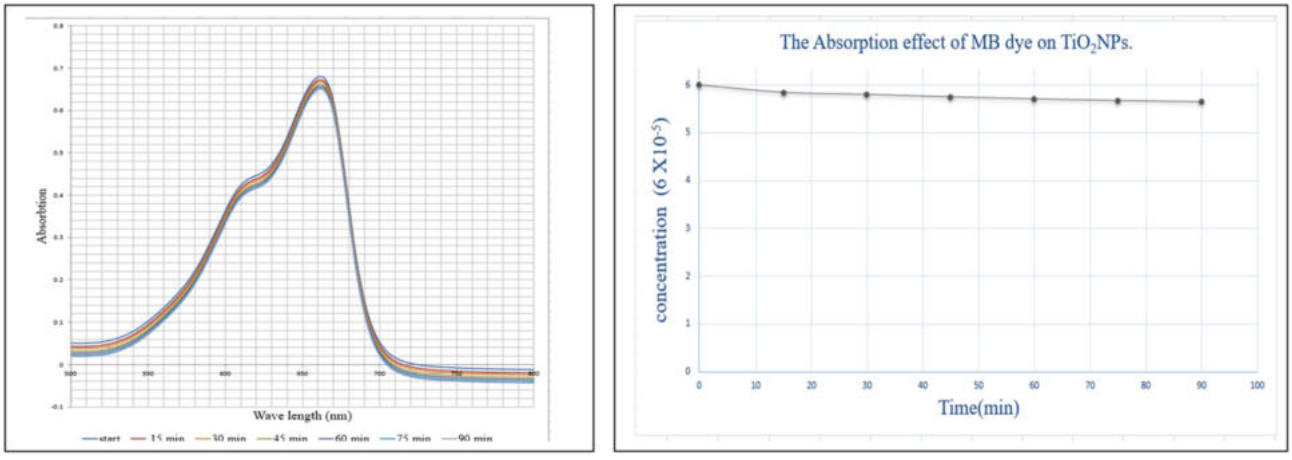

Fig. 8. Absorbance of MB dye with TiO_2NPs in the visible light region, (a) Absorbance vs wave length (nm), (b) concentration vs time.

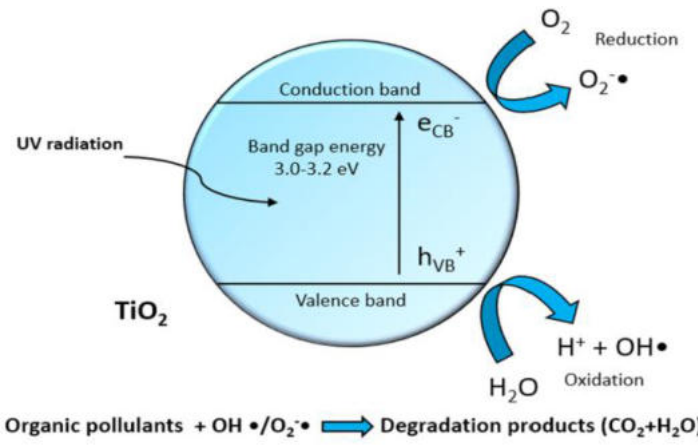

Fig. 9. Schematic photochemical activation process and bandgap for TiO_2NPs.[59]

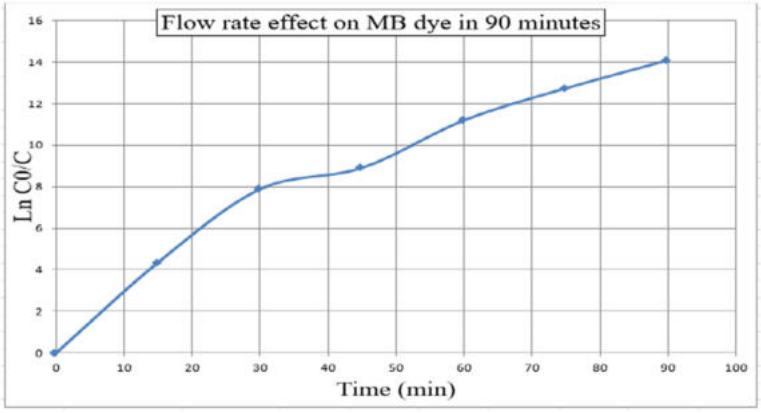

Fig. 10. Flow rate effect on MB dye in 90 min ([MB] = 20 ppm; TiO_2NPs loading = none).

to improve the photocatalyst performances, doping TiO_2NPs with heteroatoms to reduce the wide bandgap, or irradiate the TiO_2NPs with UV photons which have sufficient energy to overcome this bandgap.[58]

TiO_2NPs has a valence band (VB) filled with electrons and a conduction band (CB) with higher energy and absence of electrons, as irradiation of TiO_2NPs by UV light sources, this process induces the excitation and transition of electrons from valence band to the conduction band, this generates positive holes with the TiO_2NPs VB, these holes reduce water molecules producing free hydroxyl radicals, while the electrons in conduction band are caught by oxygen molecules, this leads to produce superoxide radicals anion, which is responsible for mineralize organic pollutants to water and carbon dioxide, as shown in Fig. 9.[59]

Flow rate effect on degradation of MB dye

The effect of flow rate on MB dye has been investigated, A 20 ppm (320 ml) of MB dye was added to the photoreactor without any irradiation, with flow rate speed = 750 mlPM, the results show decrease in concentration in 90 min, with percentage (14%) as shown in Fig. 10.

Irradiation of MB dye with different UV-light sources

Irradiation of MB dye has been investigated with different UV lamps (UV-A, UV-B, UV-C) as shown in Fig. 11. A 20 ppm (320 ml) of MB dye was added to the photoreactor, irradiation of all experiments shows that the MB dye decreases in concentration in 90 min.

The calculation of MB dye with irradiation by three types of UV light sources shows increase of photolysis in 90 min. Fig. 12 shows D% for UV-C = 34%, both UV-B and UV-A results are 29%.

Methylene blue photodegradation with photocatalyst loading

Irradiation of MB dye with loading (0.05 g) of TiO_2NPs for 90 minutes has been invistegated,[60] with different UV lamps, UV-A (365 nm), UV-B (311 nm), and UV-C (254 nm). Fig. 13a, Fig. 13b and Fig. 13c

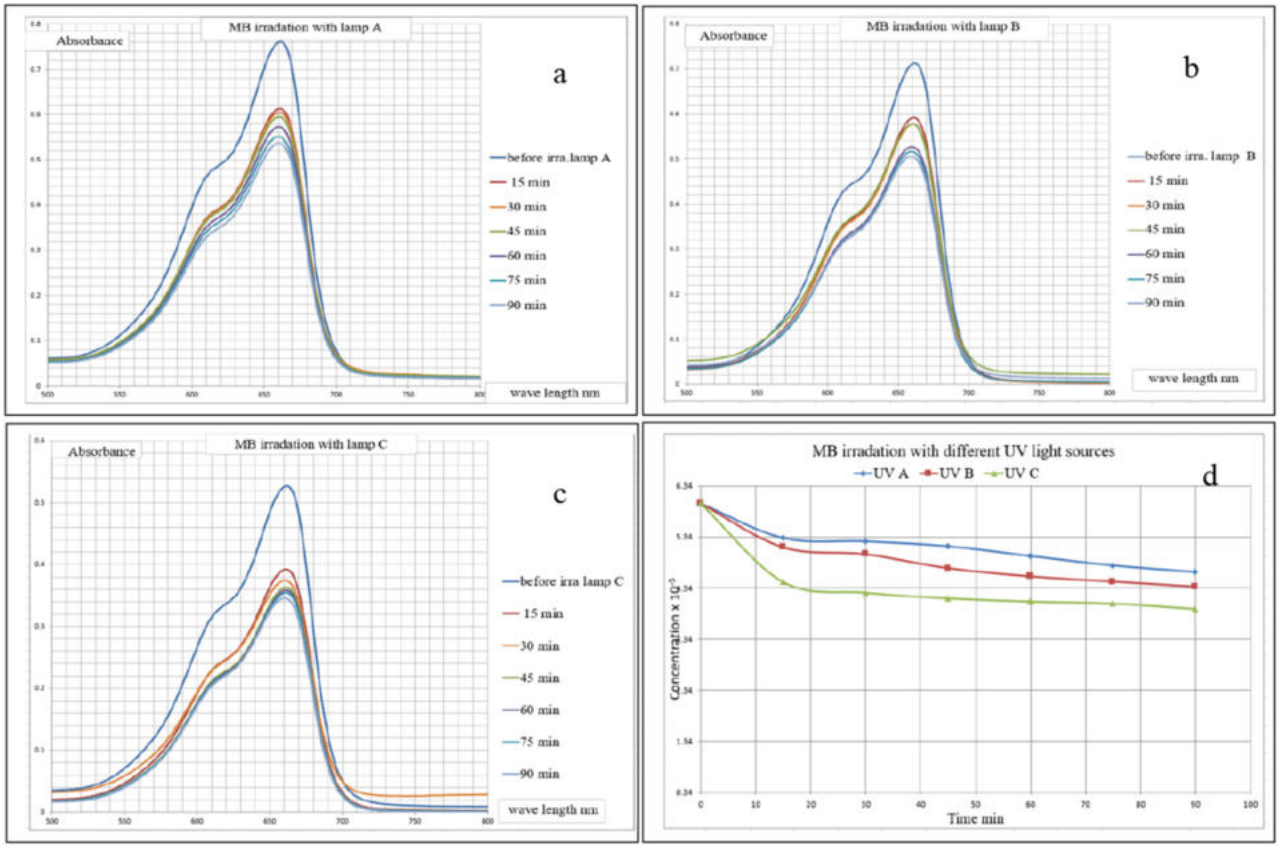

Fig. 11. MB dye irradiation with different UV lamps, (a) lamp UV-A, (b) lamp UV-B, (c) lamp UV-C, (d) shows comparing of three UV lamps in concentration decreases.

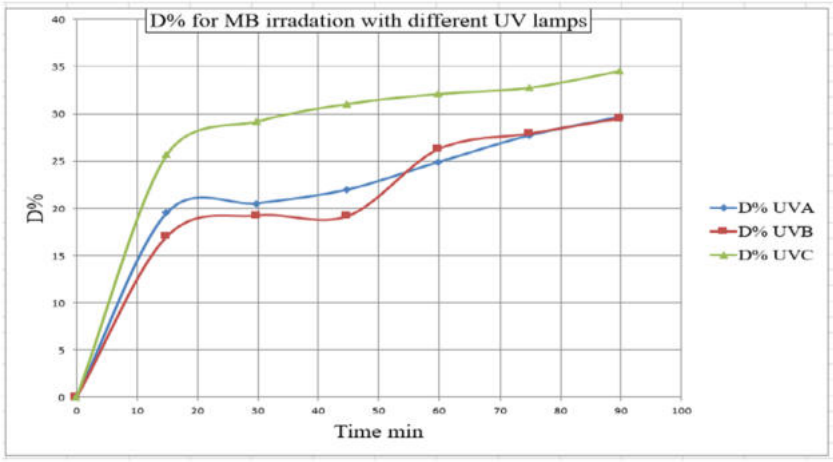

Fig. 12. D% for MB dye irradiation with different UV lamps, ([MB] = 20 ppm; TiO_2NPs loading = none).

show decrease in concentration of MB dye with time, which indicates the photodegradation process with different percentage.

This process of MB dye irradiation with loading TiO_2NPs as a catalyst is called photocatalytic, the mechanism of this process, due to the energy transfer from source of photons (UV light sources), illuminated the catalyst (TiO_2NPs). These photons excite the electrons in VB (valence band) to CB (conduction band) leaving a positive hole in VB, the energy of these photons higher than the bandgap of TiO_2NPs, these excited electrons and positive hole are responsible for producing free hydroxyl radicals, and superoxide radicals anion, which lead to breaking the

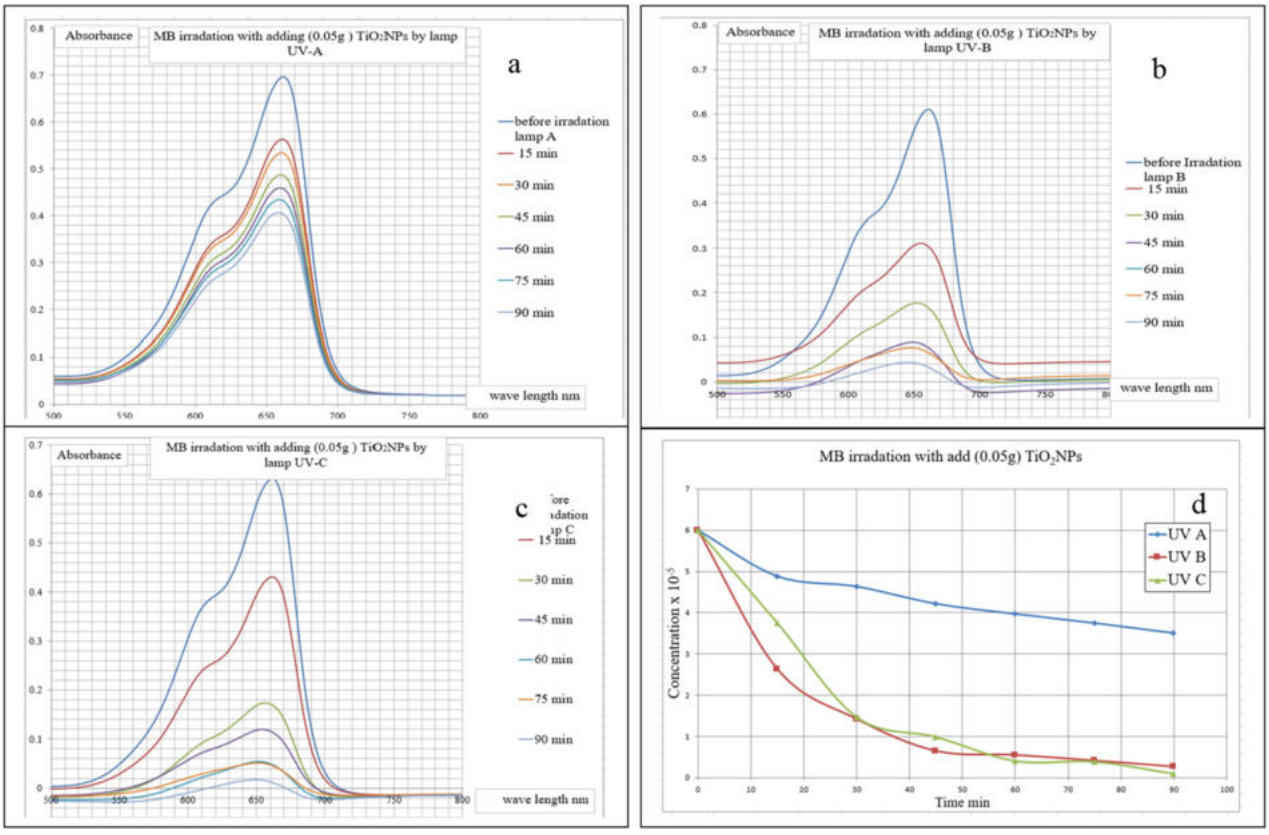

Fig. 13. MB dye irradiation with different UV lamps, (a) lamp UV-A, (b) lamp UV-B, (c) lamp UV-C, (d) shows comparing of three UV lamps in concentration decreases, ([MB] = 20 ppm; TiO_2 NPs loading = 0.05 g, Time = 90 min).

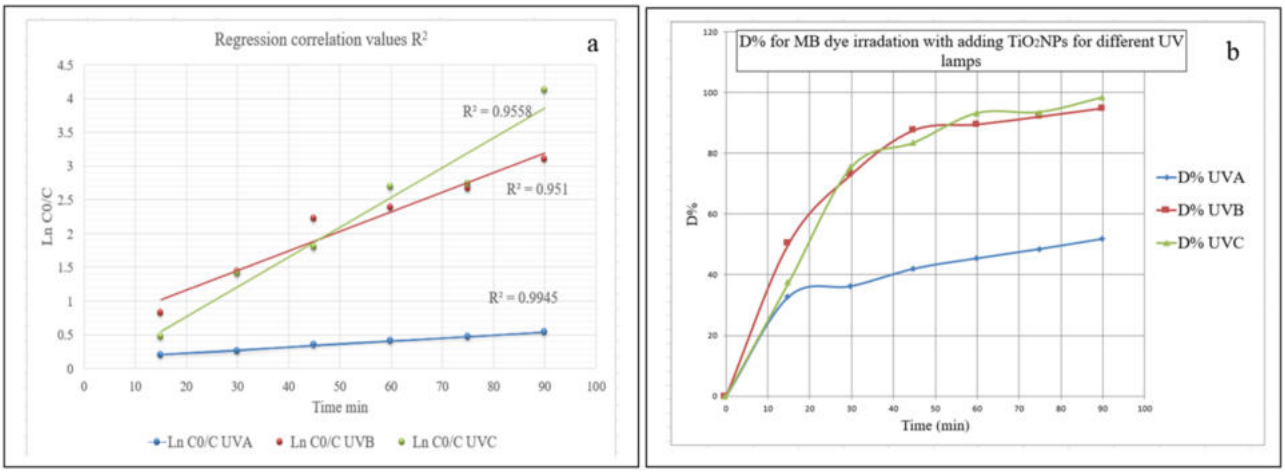

Fig. 14. (a) Graph of kinetic rate degradation showing regression correlation values R^2, (b) D% for MB irradiation with different UV lamps, all experiments ([MB] = 20 ppm; TiO_2 NPs loading = 0.05 g, Time =90 min).

chemical chains of organic pollutant, in this study MB.[61]

The degradation process follows pseudo first order kinetic reaction,[62,63] as a graph of ln (C0/C) against time was plotted as shown in Fig. 14a, a linear line shows the regression correlation value for each UV lamp which fulfilled first order kinetics.

Rate constant has been calculated, as it shows Fig. 14a, with all reactions followed a pseudo first order which is described by Eq. (2). Table 4. shows

Table 4. Rate constant and regression correlation of different UV light sources.

Regression correlation UV-A	Regression correlation UV-B	Regression correlation UV-C	K (min^{-1}) UV-A	K (min^{-1}) UV-B	K (min^{-1}) UV-C	Time (min)
0.9945	0.951	0.9558	0	0	0	0
			0.0136	0.0549	0.0313	15
			0.0085	0.0479	0.0468	30
			0.0078	0.0494	0.0400	45
			0.0068	0.0397	0.0448	60
			0.0062	0.0356	0.0364	75
			0.0059	0.0344	0.0457	90

the rate constant and regression correlation (R^2) for different UV light sources.

From Table 4, UV-C has the highest rate constant after (90 min) of irradiation, (0.0457 min^{-1}), comparing with UV-B (0.0344 min^{-1}), UV-A (0.0059 min^{-1}), which indicate the high speed of reaction, this parameter explains the high photodegradation percentage results for UV-C comparing to UV-B, and UV-A.

Fig. 14b, shows the highest degradation obtained with UV-C with 98.37% of MB dye being removed, the next best degradation is 94.9% with UV-B, while UV-A achieved 51.78% removable of MB dye.

Conclusion

In this study, rutileTiO_2NPs have been prepared using green synthesized methods using melon peel extract, the prepared nanoparticles are characterized to conform its morphology and surfaces. The new photoreactor which is designed and implemented for photodegradation process achieved excellent results, with using different UV light source UV-A, UV-B, and UV-C, and loading very small amount of TiO_2NPs powder (0.05 g) which achieved with UV-C (98.37%) photodegradation of MB dye, while UV-B achieved (94.9%) photodegradation, and UV-A achieved (51.78%) photodegradation. All experiments were carried out in 90 min. UV-C irradiation shows faster photodegradation process, which indicates its capability roles in photolysis, as it has a shorter penetration wave length and high energy level. Degradation study of MB dye shows that the reaction follows first order kinetic reaction, a graph of ln (C0/Ct) against time was plotted to show the regression correlation R^2, and rate constant for different UV light sources.

Acknowledgment

The authors are grateful to the Department of Chemistry, College of Science/University of Baghdad for providing the chemicals and tools throughout the research.

Authors' declaration

- Conflicts of Interest: None.
- We hereby confirm that all the Figures and Tables in the manuscript are ours. Furthermore, any Figures and images, that are not ours, have been included with the necessary permission for republication, which is attached to the manuscript.
- No animal studies are present in the manuscript.
- No human studies are present in the manuscript.
- Ethical Clearance: The project was approved by the local ethical committee at University of Baghdad.

Authors' contribution statement

M.A.H. and W.N.A. designed the study of Synthesis, characterization and photodegradation study of titanium oxide nanoparticles that prepared using Melon peel for photodegradation of Methelene blue dye, all experiment done with supervision of W.N.A, M.A.H and W.N.A wrote the paper with data analysis and drafting the research.

References

1. Joudeh N, Linke D. Nanoparticle classification, physicochemical properties, characterization, and applications: A comprehensive review for biologists. J Nanobiotechnology. 2022;20(1):262. https://doi.org/10.1186/s12951-022-01477-8.
2. Mekuye B, Abera B. Nanomaterials: An overview of synthesis, classification, characterization, and applications. Nano Select. 2023;4(8):486–501. https://doi.org/10.1002/nano.202300038.
3. Griffo R, Di Natale F, Minale M, Sirignano M, Parisi A, Carotenuto C. Analysis of carbon nanoparticle coatings via wettability. Nanomaterials. 2024;14(3):301. https://doi.org/10.3390/nano14030301.
4. Abdelkalik Hussain M, Al Sieadi WN. Green synthesized titanium dioxide nanoparticles from date seed for photocatalytic dye degradation. Iraqi J Sci. 2025;66(11):4679–4694. https://doi.org/10.24996/ijs.2025.66.11.1.
5. Chumsard W, Fawcett D, Fung CC, Poinern GEJ. Biogenic synthesis of gold nanoparticles from waste watermelon and their antibacterial activity against Escherichia coli and staphylococ-

cus epidermidis. Int. J. Res. Med. Sci. 2019;7(7):2499–2505. http://dx.doi.org/10.18203/2320-6012.ijrms20192874.
6. Masood MM, Al Sieadi WN. Eco-friendly synthesis of nickel oxide nanoparticles using licorice leaves extract for anticancer effect against bone cancer cells MG-63 and antibacterial activity. Iraqi J Sci. 2025;66(9):3635–3654. https://doi.org/10.24996/ijs.2025.66.9.12.
7. Teimoori S, Shirkhanloo H, Hassani AH, Panahi M, Mansouri N. New extraction of toluene from water samples based on nanocarbon structure before determination by gas chromatography. Int. J. Environ. Sci. 2023;20:6589–6608. https://doi.org/10.1007/s13762-023-04906-9.
8. Ijaz I, Gilani E, Nazir A, Bukhari A. Detail review on chemical, physical and green synthesis, classification, characterizations and applications of nanoparticles. Green Chem Lett Rev. 2020;13(3):59–81. https://doi.org/10.1080/17518253.2020.1802517.
9. Baig N, Kammakakam I, Falath W. Nanomaterials: A review of synthesis methods, properties, recent progress, and challenges. Mater Adv J. 2021;2(6):1821–1871. https://doi.org/10.1039/d0ma00807a.
10. Alaallah NJ, Dhahir SA, Ali HH. Determination of sulfacetamide sodium in pure and their pharmaceutical formulations by using cloud point extraction method. Baghdad Sci J. 2021;18(3):575–582. https://doi.org/10.21123/BSJ.2021.18.3.0575.
11. Al-darwesh MY, Ibrahim SS, Mohammed MA. A review on plant extract mediated green synthesis of zinc oxide nanoparticles and their biomedical applications. Results Chem. 2024;101368. https://doi.org/10.1016/j.rechem.2024.101368.
12. El Shafey AM. Green synthesis of metal and metal oxide nanoparticles from plant leaf extracts and their applications: A review. Green Process Synth. 2020;9(1):304–339. https://doi.org/10.1515/gps-2020-0031.
13. Osman AI, Zhang Y, Farghali M, Rashwan AK, Eltaweil AS, El-monaem EM, *et al.* Synthesis of green nanoparticles for energy, biomedical, environmental, agricultural, and food applications: A review. Environ Chem Lett. 2024;22:841–887. https://doi.org/10.1007/s10311-023-01682-3.
14. Singh H, Desimone MF, Pandya S, George N, Adnan M, Aldarhami A, *et al.* Revisiting the green synthesis of nanoparticles: Uncovering influences of plant extracts as reducing agents for enhanced synthesis efficiency and its biomedical applications. Int J Nanomedicine. 2023;18:4727–4750. https://doi.org/10.2147/IJN.S419369.
15. Habeeb Rahuman HB, Dhandapani R, Narayanan S, Jasani S, George N, Adnan M, *et al.* Medicinal plants mediated the green synthesis of silver nanoparticles and their biomedical applications. IET Nanobiotechnol. 2022;16(4):115–144. https://doi.org/10.1049/nbt2.12078.
16. Antunes Filho S, Dos Santos MS, Dos Santos O, Backx B, Soran M, Opris O, *et al.* Biosynthesis of nanoparticles using plant extracts and essential oils. Molecules. 2023;28(7):3060. https://doi.org/10.3390/molecules28073060.
17. Some S, Das S, Mondal R, Gangopadhyay M, Basak G. Medicinal plant extract mediated green synthesis of metallic nanoparticles: A review. Int J Plant Env PE. 2021;7(2):119–132. https://doi.org/10.18811/ijpen.v7i02.02.
18. Syamsol Bahri S, Harun Z, Hubadillah K, Wansalleh W, Rosman N, Kamaruddin N, *et al.* Review on recent advance biosynthesis of TiO_2 nanoparticles from plant-mediated materials: Characterization, mechanism and application. IOP Conf Ser Mater Sci Eng. 2021;1142(1):012005. https://doi.org/10.1088/1757-899x/1142/1/012005.
19. Sathishkumar P, Gu FL, Zhan Q, Palvannan T, Yusoff AM. Flavonoids mediated 'Green' nanomaterials: A novel nanomedicine system to treat various diseases – Current trends and future perspective. Mater Lett. 2018;210:26–30. https://doi.org/10.1016/j.matlet.2017.08.078.
20. Tadioto V, Giehl A, Cadamuro RD, Guterres I, Santos A, Bressan S, *et al.* Bioactive compounds from and against yeasts in the one health context: A comprehensive review. Fermentation. 2023;9(4):363. https://doi.org/10.3390/fermentation9040363.
21. Xie Y, Peng Q, Ji Y, Xie A, Yang L, Mu S, *et al.* Isolation and identification of antibacterial bioactive compounds from bacillus megaterium L2. Front Microbiol. 2021;12:645484. https://doi.org/10.3389/fmicb.2021.645484.
22. Rousta N, Aslan M, Yesilcimen Akbas M, Ozcan F, Sar T, Taherzadeh M. Effects of fungal based bioactive compounds on human health: Review paper. Crit Rev Food Sci Nutr. 2024;64(20):7004–7027. https://doi.org/10.1080/10408398.2023.2178379.
23. Zahra Z, Habib Z, Chung S, Badshah M. Exposure route of TiO_2 Nps from industrial applications to wastewater treatment and their impacts on the agro-environment. Nanomaterials. 2020;10(8):1–22. https://doi.org/10.3390/nano10081469.
24. Abass AK, Al Sieadi WNJ, Al-Sammarraie AKMA. Investigation of the electrical, compositional, and magnetic features of hybrid lead oxide nanocomposites. Eurasian Chem Commun. 2022;4(11):1044–1053. https://doi.org/10.22034/ecc.2022.344547.1479.
25. Dincheva I, Badjakov I, Galunska B. New insights into the research of bioactive compounds from plant origins with nutraceutical and pharmaceutical potential. Plants. 2023;12(2):258. https://doi.org/10.3390/plants12020258.
26. Loi M, Paciolla C, Logrieco AF, Mulè G. Plant bioactive compounds in pre- and postharvest management for aflatoxins reduction. Front Microbiol. 2020;11(3):243. https://doi.org/10.3389/fmicb.2020.00243.
27. Tsakni A, Chatzilazarou A, Tsakali E, Tsantes AG, Impe JV, Houhoula D. Identification of bioactive compounds in plant extracts of Greek flora and their antimicrobial and antioxidant activity. Separations. 2023;10(7):373. https://doi.org/10.3390/separations10070373.
28. Stéphane F, Jules B, Batiha G, Ali I, Bruno L. Extraction of bioactive compounds from medicinal plants and herbs. Natural Medicinal Plants. Intech Open. 2022. https://doi.org/10.5772/intechopen.98602.
29. Sytar O, Smetanska I. Special issue "Bioactive compounds from natural sources (2020, 2021)". Molecules. 2022;27(6):1929. https://doi.org/10.3390/molecules27061929.
30. Kussmann M, Abe Cunha DH, Berciano S. Bioactive compounds for human and planetary health. Front Nutr. 2023;17(10):1193848. https://doi.org/10.3389/fnut.2023.1193848.
31. Rana A, Yadav K, Jagadevan S. A comprehensive review on green synthesis of nature-inspired metal nanoparticles: Mechanism, application and toxicity. J Clean Prod. 2020;272:122880. https://doi.org/10.1016/j.jclepro.2020.122880.
32. Rolim PM, Fidelis GP, Padiha CE, Santos ES, Rocha HA. Phenolic profile and antioxidant activity from peels and seeds of melon (*Cucumis melo L.* var. reticulatus) and their antiproliferative effect in cancer cells. Braz J Med Biol Res. 2018;51(4):6069. https://doi.org/10.1590/1414-431$\times$20176069.

33. Mallek-Ayadi S, Bahloul N, Baklouti S, Kechaou N. Bioactive compounds from Cucumis melo L. fruits as potential nutraceutical food ingredients and juice processing using membrane technology. Food Sci Nutr. 2022;10(9):2922–2934. https://doi.org/10.1002/fsn3.2888.
34. Rani P, Kumar N, Perinmbam K, Devanesan S, Alsalhi M, Asemi N, *et al.* Synthesis of silver nanoparticles by leaf extract of cucumis melo L. and their In Vitro antidiabetic and anticoccidial activities. Molecules. 2023;28(13):4995. https://doi.org/10.3390/molecules28134995.
35. Ying Qian O, Harith S, Razif Shahril M, Shahidan N. Bio active compounds in Cucumis Melo L. and its beneficial health effects: A scoping review. Malays App Biol. 2019;48(4):11–23.
36. Rasu V, Krishnasamy K. Green synthesis of silver nanoparticles and its characterization using cucumis Melo L. Fruit Extract. 2020;5(5):99–103.
37. Archana P, Janarthanan B, Bhuvana S, Rajiv P, Sharmila S. Concert of zinc oxide nanoparticles synthesized using Cucumis melo by green synthesis and the antibacterial activity on pathogenic bacteria. Inorg Chem Commun. 2022;137:109255. https://doi.org/10.1016/J.INOCHE.2022.109255.
38. Dharma HNC, Jaafar J, Widiastuti N, Matsuyama H, Rajabsadeh S, Othman MHD, *et al.* A review of titanium dioxide (TiO2)-based photocatalyst for oilfield-produced water treatment. Membranes. 2022;12(3):345. https://doi.org/10.3390/membranes12030345.
39. Ali SF, Seaidi WNA, Ani KEA. Study of thermal degradation of plasticized poly (4-ethoxystyrene) in solution and solid films. Int J Pharm Res. 2020;12(3):436–444. https://doi.org/10.31838/ijpr/2020.12.03.067.
40. El Sharkawy HM, Shawky AM, Elshypany R, Selim H. Efficient photocatalytic degradation of organic pollutants over TiO_2 nanoparticles modified with nitrogen and M_oS_2 under visible light irradiation. Sci Rep. 2023;13(1):8845. https://doi.org/10.1038/s41598-023-35265-7.
41. Ghosh M, Chowdhury P, Ray AK. Photocatalytic activity of aeroxide TiO_2 sensitized by natural dye extracted from mangosteen peel. Catalysts. 2020;10(8):917. https://doi.org/10.3390/catal10080917.
42. Goutam SP, Saxena G, Singh V, Yadav AK, Bharagava RN, Thapa KB. Green synthesis of TiO_2 nanoparticles using leaf extract of Jatropha curcas L. for photocatalytic degradation of tannery wastewater. Chem Eng. 2018;336:386–396. https://doi.org/10.1016/j.cej.2017.12.029.
43. Xu J, Zhang T, Zhang J. Photocatalytic degradation of methylene blue with spent FCC catalyst loaded with ferric oxide and titanium dioxide. Sci Rep. 2020;10(1):12730. https://doi.org/10.1038/s41598-020-69643-2.
44. Alkaykh S, Mbarek A, Ali-Shattle EE. Photocatalytic degradation of methylene blue dye in aqueous solution by $MnTiO_3$ nanoparticles under sunlight irradiation. Heliyon. 2020;6(4):3663. https://doi.org/10.1016/j.heliyon.2020.e03663.
45. Geetha G V, Sivakumar R, Sanjeeviraja C, Ganesh V. Photocatalytic degradation of methylene blue dye using $ZnWO_4$ catalyst prepared by a simple co-precipitation technique. J Solgel Sci Technol. 2021;97(3):572–580. https://doi.org/10.1007/s10971-021-05480-7.
46. Nakayama T, Honda R, Kuwata K, Usui S, Uno B. Electrochemical and mechanistic study of reactivities of α-, β-, γ-, and δ-tocopherol toward electrogenerated superoxide in N, N-dimethylformamide through proton-coupled electron transfer. Antioxidants. 2022;11(1):9. https://doi.org/10.3390/antiox11010009.
47. Iqbal J, Abbasi BA, Yaseen T, Zahra SA, Shahbaz A, Shah SA, *et al.* Green synthesis of zinc oxide nanoparticles using Elaeagnus angustifolia L. leaf extracts and their multiple in vitro biological applications. Sci Rep. 2021;11(1):20988. https://doi.org/10.1038/s41598-021-99839-z.
48. Lal M, Sharma P, Ram C. Calcination temperature effect on titanium oxide (TiO_2) nanoparticles synthesis. Optik (Stuttg). 2021;241(2):166934. https://doi.org/10.1016/j.ijleo.2021.166934.
49. Kim MG, Kang JM, Lee JE, Kim KS, Kim KH, Cho M, *et al.* Effects of calcination temperature on the phase composition, photocatalytic degradation, and virucidal activities of TiO_2 nanoparticles. ACS Omega. 2021;6(16):10668–10678. https://doi.org/10.1021/acsomega.1c00043.
50. Kaiba A, Ouerghi O, Geesi MH, Elsanousi A, Belkacem A, Dehbi O, *et al.* Characterization and catalytic performance of Ni-Doped TiO_2 as a potential heterogeneous nanocatalyst for the preparation of substituted pyridopyrimidines. J Mol Struct. 2020;(1203):127367. https://doi.org/10.1016/j.molstruc.2019.127376.
51. Sahadat M, Ahmed S. Easy and green synthesis of TiO2 (anatase and rutile): Estimation of crystallite size using scherrer equation, williamson-hall plot, monshi-scherrer model, size-strain plot, Halder-Wagner model. Results Mater. 2023;(20):100492. https://doi.org/10.1016/j.rinma.2023.100492.
52. Ahmadiasl R, Moussavi G, Shekoohiyan S, Razavian F. Synthesis of Cu-Doped TiO2 Nanocatalyst for the enhanced photocatalytic degradation and mineralization of gabapentin under UVA/LED irradiation: Characterization and photocatalytic activity. Catalysts. 2022;12(11):1310. https://doi.org/10.3390/catal12111310.
53. Li X, Gao Y, Xiong H, Yang Z. The electrochemical redox mechanism and antioxidant activity of polyphenolic compounds based on inlaid multi-walled carbon nanotubes-modified graphite electrode. Open Chem. 2021;19(1):961–973. https://doi.org/10.1515/chem-2021-0087.
54. Rambabu K, Bharath G, Banat F, Show PL. Biosorption performance of date palm empty fruit bunch wastes for toxic hexavalent chromium removal. Environ Res. 2020;(187):109694. https://doi.org/10.1016/j.envres.2020.109694.
55. Al Ani, Ramadhan AE, AlSieadi WN. Fourier-transform infrared spectroscopic study of plasticization effects on the photodegradation of poly(fluorostyrene) isomers films. J Vinyl Addit Technol. 2018;24(1):75–83. https://doi.org/10.1002/vnl.21529.
56. Baker WB, Parthasarathy AB, Busch DR, Mesquita RC, Greenberg JH, Yodh AG. Modified beer-lambert law for blood flow. Biomed Opt Express. 2014;5(11):4053–4075. https://doi.org/10.1364/boe.5.004053.
57. Safeen A, Safeen K, Ullah R, Zulfqar, Shah WH, Zaman Q, *et al.* Enhancing the physical properties and photocatalytic activity of TiO2 nanoparticles via cobalt doping. RSC Adv. 2022;12(25):15767–15774. https://doi.org/10.1039/d2ra01948e.
58. Dimo SN, Obidi OF, Nejo AO, Olaleru SA, Ejidike LP, Adetona AJ. Biofabrication, spectroscopic, and photocatalytic studies of titania nanoparticles mediated by Proteus mirabilis strain NG-ABK-32 for smart applications. Smart Sci. 2024;(12):373–386. https://doi.org/10.1080/23080477.2024.2338651.
59. Rosa D, Abbasova N, Di Palma L. Titanium dioxide nanoparticles doped with iron for water treatment via Photocatalysis: A review. Nanomaterials. 2024;14(3):293. https://doi.org/10.3390/nano14030293.
60. Fatimah I, Fahrani D, Harmawantika T, Sahroni I, Kamari A, Rahmatilla CS, *et al.* Functionalization of hydroxyapatite derived from cockle (Anadara granosa) shells into hydroxyapatite–nano TiO_2 for photocatalytic degradation of methyl violet. Sustain Environ Res. 2019;1(1):29–40. https://doi.org/10.1186/s42834-019-0034-3.

61. Utami FD, Rahman DY, Margareta DO, Rahmayanti HD, Munir R, Sustint E, *et al.* TiO_2 photocatalytic degradation of methylene blue using simple spray method. IOP Conf Ser Mater Sci Eng. 2019;599(1):012026. https://doi.org/10.1088/1757-899X/599/1/012026.
62. Abdelkalik Hussain M, Al Sieadi WN. Determination and removal of methylene blue dye via photodegradation using titanium dioxide nanoparticles from watermelon rind. Anal Methods Environ Chem J. 2025;8(1):26–38. https://doi.org/10.24200/amecj.v8.i01.362.
63. Rakhtshah J, Shirkhanloo H, Esmaeili N. A rapid extraction of toxic styrene from water and wastewater samples based on hydroxyethyl methylimidazolium tetrafluoroborate immobilized on MWCNTs by ultra-assisted dispersive cyclic conjugation-micro-solid phase extraction. Microchem. J. 2021;170:106759. https://doi.org/10.1016/j.microc.2021.106759.

تحضير وتشخيص ودراسة التحلل الضوئي لجزيئات ثنائي أوكسيد التيتانيوم النانوية باستخدام مستخلص قشر البطيخ

محمد عبد الخالق حسين، وضاح ناجي السعيدي

قسم الكيمياء، كلية العلوم، جامعة بغداد، بغداد، العراق.

الخلاصة

تلعب تقنية النانو دوراً مهماً في حماية البيئة، مع تطبيقاتها المتعددة منها على سبيل المثال، التخليق الخضري للجسيمات النانوية باستخدام بقايا اجزاء النباتات، كذلك، يظهر تطبيق التحفيز الضوئي باستخدام أشباه الموصلات النانوية تأثيراً واضحاً في حماية البيئة من حيث معالجة المياه من الملوثات العضوية . تجمع هذه الدراسة بين هذين التطبيقين، من حيث التخليق الأخضر لجسيمات ثاني أكسيد التيتانيوم النانوية (TiO2NPs) باستخدام قشر البطيخ (*Cucumis melo* L) بطريقة السول جل، وكذلك التحلل الضوئي لصبغة الميثيلين الزرقاء باستخدام جهاز مفاعل ضوئي جديد للإشعاع تم تصميمه وتنفيذه لهذا الغرض. يُستخدم هذا الجهاز لتشعيع صبغة الميثيلين الزرقاء بثلاث أنواع مختلفة من مصادر الضوء فوق البنفسجي لدراسة التحلل الضوئي في حالات مختلفة، أولاً عند دوران صبغة الميثيلين الزرقاء في الجهاز فقط، وثانيًا عند تشعيع صبغة الميثيلين الزرقاء باستخدام الأشعة فوق البنفسجية-A، والأشعة فوق البنفسجية-B، والأشعة فوق البنفسجيةUV-C مع الدوران، وأخيرا تأثير إضافة (0.05 جرام) من مسحوق TiO2NPs مع التشعيع والتدوير بصبغة الميثيلين الزرقاء في المفاعل. نسبة مختلفة من إزالة صبغة الميثيلين الزرقاء تم الوصول اليها. تم تشخيص جسيمات TiO2NPs باستخدام تحليل تشتت الطاقة (EDX)، التحليل الطيفي للأشعة فوق البنفسجية والمرئية (UV-Vis)، المجهر الإلكتروني الماسح (SEM)، التحليل الطيفي للأشعة تحت الحمراء (FTIR)، التحليل الطيفي للأشعة السينية (XRD)، التحليل الطيفي الذري المجهري (AFM). تم تسجيل نسبة عالية من للتحلل الضوئي تحت الأشعة فوق البنفسجية - C والأشعة فوق البنفسجية - B لصبغة MB في 90 دقيقة.

الكلمات المفتاحية: التخليق الخضري، قشر البطيخ، صبغة الميثيلين الزرقاء، التحلل الضوئي، جسيمات اوكسيد التيتانيوم النانوية.